

LOW TEMPERATURE SIMULATION OF AMMONIA REFRIGERATION BASED ON DISSIPATIVE MOLECULAR DYNAMICS

by

Xiao-Yan LIU^a, Yang YANG^a, Hai-Qian ZHAO^{a*}, Ying XU^a, and Shu CHEN^b,

^a School of Mechanical Science and Engineering,
Northeast Petroleum University, Daqing, Heilongjiang, China

^b Petrochina Tarim Oilfield Company, Korla, Xinjiang, China

Original scientific paper

<https://doi.org/10.2298/TSCI220819169L>

To solve the problem of heat resistance of the oil film in the evaporator pipe-line of the ammonia refrigeration system, it is extremely important to study the interaction mechanism of the oil/ammonia system. The method of dissipative molecular dynamics is used to simulate the oil/ammonia flow state at different temperatures and concentrations, and the mechanism of its interaction was analyzed. It was also found that various parameters are greatly affected by temperature in the research process, the linear relationship of temperature on various parameters was quantitatively calculated. The oil/ammonia system were divided into emulsion and layered liquid. The oil phase (or ammonia phase) with low percentage at low temperature all exists in the form of droplets. The oil-ammonia interfacial tension first increases and then decreases with the increase of oil content. At the same temperature, the interfacial tension reached its maximum when the oil content was 70%. The oil percentage of 30% concentration was the phase inversion point. When the oil percentage was 30-70%, the oil and ammonia two-phases were stratified, and the oil adhered to the surface of the pipe wall. Therefore, the heat transfer performance of the system was the worst when the oil content was 30-70%. As the temperature increased, the interaction parameter a_{ij} decreased significantly. The linear relationship between χ and $1/T$ was very consistent with the Flory-Huggins mean field theory. This linear equation provided a basis for subsequent related research.

Key words: ammonia refrigeration oil/ammonia system dissipative particle dynamics, temperature effect

Introduction

Ammonia as a green natural refrigerant, with very good thermodynamic properties, ammonia unit standard refrigeration capacity of about 2175.68 kJ/m³, COP in different units can reach 3.4-3.7. The price of ammonia is relatively cheap and has certain energy-saving characteristics. Ammonia also has obvious environmental characteristics, with zero ozone depletion potential (ODP) [1] and zero GWP [2], which can mitigate the effects of global warming. At present, the research on ammonia refrigeration has gradually become the research hot spot of the industry [3]. Lubricants are an important part of refrigeration systems, but they can have a greater impact on the performance of refrigeration systems [4]. The lubricants oil that flows out of the compressor adheres to the surface to form an oil film as it flows through the evaporator

* Corresponding author, e-mail: dqzhaohaiqian@163.com

pipe. When the viscosity of the oil film is very large, the flow rate of refrigerant vapor is not sufficient to take these lubricants out of the evaporator. This is accumulated in the evaporator, which in turn affects the cooling equipment heat exchange effect [5]. Thus it can be seen that the intersolution capacity of lubricants and refrigerants is very important, in order to make the two better mutually soluble, the relevant scholars have developed a higher mutual solubility with ammonia synthetic lubricants, which greatly solves the problem of ammonia refrigeration system due to refrigerant and lubricant insoluble. However, due to special conditions in the evaporator, the refrigerant/oil mixture remains in the evaporator. There is the phenomenon of lubricant adhesion to the pipe wall [6]. In order to improve the heat exchange efficiency on this basis, the mathematicians studied the performance of the heat exchanger and the boiling heat exchange of the pipe [7, 8]. Although this improves the evaporator heat exchange, but the oil layer caused by lubricant obstruction heat exchange problem has not been fundamentally resolved. At the same time, most scholars focus on the problem of oil retention in evaporators, mainly study oil ammonia separators, but oil ammonia separation in the refrigeration unit is too complex, installation, maintenance and service life are problems [9]. To solve the problem of evaporator oil retention, the most fundamental is to understand the mechanism of oil/ammonia in the evaporator interaction and its flow pattern. Simulation can provide the dynamic details and time-dependent evolution of the structure [10], which is difficult or impossible to obtain through experimental methods. This information helps to understand the interface behaviors in the oil/ammonia system. Dissipative molecular dynamics (DPD) is a coarse-grained simulation method [11]. The DPD can provide equilibrium thermodynamic properties, therefore, the simulation is used in this research and combined with Materials Studio 2019 software. Dissipative molecular dynamics is used to study the interaction mechanisms between lubricating oil and liquid ammonia at low temperature. The liquid phase state of the lower oil/ammonia at different temperatures and oil content is simulated and the interfacial tension is used for quantitative calculations. A qualitative analysis of the oil/ammonia interaction in the evaporator and its flow pattern. In DPD simulation, the repulsive force parameter is the key parameter to obtain interfacial tension. But for ammonia refrigeration, DPD calculation data is not systematically given by scholars. Therefore, a method based on DPD kinetics is provided in this study to obtain the correspondence between the Flory-Huggins parameter χ and the excess repulsive force parameter Δa at different temperatures and they are applied to calculate the repulsive force parameters. This provides theoretical basis and data information for follow-up research.

Method

Dissipative molecular dynamics fundamental equations and actions

In DPD simulation, beads represented the basic chemical properties of molecules and influenced each other by effectively affecting potentials. The force between pairs of beads was determined by conservative force, dissipative force and random force:

$$F_i = \sum_{j \neq i} (F_{ij}^C + F_{ij}^D + F_{ij}^R) \quad (1)$$

where F_{ij}^C was the conservative force, F_{ij}^D was the dissipation force, and F_{ij}^R was the random force exerted by the j bead on the i bead:

$$F_{ij}^C = a_{ij} \omega^C(r_{ij}) \hat{r}_{ij} \quad (2)$$

$$F_{ij}^D = \zeta \omega^D(r_{ij}) (V_{ij} \hat{r}_{ij}) \hat{r}_{ij} \quad (3)$$

$$F_{ij}^R = \sigma \omega^R(r_{ij}) \xi_{ij} \Delta t^{-(1/2)} \hat{r}_{ij} \quad (4)$$

where a_{ij} is the conservative force parameter, γ_{ij} – the friction factor, σ_{ij} – the defines the fluctuation amplitude, namely noise parameter, $\omega^D r_{ij}$ and $\omega^R r_{ij}$ are weight functions. The $\omega^D r_{ij}$ and $\omega^R r_{ij}$ follow a certain relation according to the fluctuation-dissipation theorem, the ω is the noise amplitude and ξ_{ij} is a random number with zero mean and unit variance, again chosen independently for each pair of interacting particles and at each timestep. The appearance of $\Delta t^{1/2}$ in this expression will be discussed below.

In the DPD method, soft spherical beads represented clusters of several single atoms or molecules or a certain volume of fluid, and had potential properties of molecules. In the case of macromolecules, multiple beads were connected together by a harmonic spring with constant k_S [12]. Similar to the MD simulation, the time evolution of the multi-body system was controlled by the Newton equations to control the motion in the DPD, which was used to estimate the trajectory of the DPD beads [13]. In addition the aforementioned forces, for polymer or chain systems, additional forces F_{ij}^{Bond} Bond due to bonding should also be included. The binding force was described [14]:

$$F_{ij}^{\text{Bond}} = -k_S (r_{ij} - r_0) \hat{r}_{ij} \quad (5)$$

where k_S is the spring constant and r_0 is the balance spring distance.

Model

First of all, the model system was constructed, the solvent beads and oil beads were first established as shown in fig. 1.

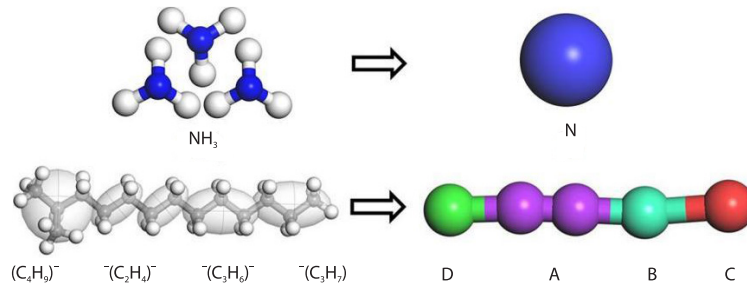


Figure 1. The coarse grained molecules of ammonia and oil

The number of liquid ammonia molecules, N_m , determined the size of the beads, where N_m represented the coarse particle size [15]. In this simulation, every 3 ammonia molecules constituted a bead. Therefore, $N_m = 3$. The molecular weight of ammonia molecule was 17 g/mol [17]. Therefore, the parameters of liquid ammonia could be calculated by the following eqs. (6)-(7) [16]:

$$V_b = N_m V_{\text{ammonia}} \quad (6)$$

$$m = N_m m_{\text{ammonia}} \quad (7)$$

According to eqs. (6)-(7), m refers to the mass of the beads; m_{ammonia} is the molecular mass of ammonia. You need to specify the bead radius in Materials Studio. The diameter of beads composed of N_m ammonia molecules is defined by the following eqs. (8)-(9) [17]:

$$r_c^3 = \rho N_m V_{\text{ammonia}} \quad (8)$$

$$r_c = (\rho N_m V_{\text{ammonia}})^{1/3} = (\rho N_m 30)^{1/3} = 3.107(\rho N_m)^{1/3} \quad (9)$$

The time scale (τ) used in the DPD calculation can be determined as follows eq. (10) [18]:

$$\tau = 14.1 N_m^{5/3} \quad (10)$$

where ρ represents the number of beads per r_c^3 , r_c represents the diameter of the beads, which was used as the length ratio, and ρ was defined as the number density of beads. In the simulation, the number density of beads was a free parameter, but considering that the interaction between beads corresponded to a linear increase in the number density of beads, and calculated the square of the number density of CPU time required per time step and per unit volume. Therefore, it was most economical to take the minimum value $\rho = 3$ within the range of reasonable bead number density [20, 21]. Therefore, in this paper, $\rho = 3$:

$$\chi_{ij} = \frac{V_{\text{ref}} (\delta_i - \delta_j)^2}{RT} \quad (11)$$

where V_{ref} was a parameter, usually the molar volume of a certain component was selected, and then the molar volume of each component of the system calculated by the Forcite module. At this time, the relationship between the Flory-Huggins parameter and the rejection parameter was:

$$a_{ij} = 3.27 \chi_{ij} + 25 \quad (12)$$

It could be found from the polymer manual that the solubility parameters of ethyl, propyl and isobutane were $10.02 \text{ (J/cm}^3)^{0.5}$, $13.091 \text{ (J/cm}^3)^{0.5}$, and $14.027 \text{ (J/cm}^3)^{0.5}$, which could be seen in the calculation. The result was very similar to this laboratory. Through the previous formulas and tab. 1, the following repulsion parameters were obtained, and the a_{ij} used in DPD calculation was shown in tab. 1.

Table 1. The repulsion parameters, a_{ij} , calculated from Flory-Huggins χ_{ij} parameters

a_{ij}	A(C ₂ H ₄)	B(C ₃ H ₆)	C(C ₃ H ₇)	D(C ₄ H ₉)	E(H ₂ O)
A(C ₂ H ₄)	25	–	–	–	–
B(C ₃ H ₆)	25.37	25	–	–	–
C(C ₃ H ₇)	25.41	25	25	–	–
D(C ₄ H ₉)	25.98	25.11	25.91	25	–
N(NH ₃)	66.03	57.16	56.91	59.91	25

The aforementioned table was obtained as the simulated force field parameters, and then the Amorphous Cell module was used to construct a box with a dimension of $80 \text{ \AA} \times 80 \text{ \AA} \times 120 \text{ \AA}$, and to enter the operating conditions in the ammonia refrigeration evaporator. All subsequent calculations were carried out using the Mesocite module in the Materials Studio 2019 software package.

In order to quantify the accuracy of the flow model, the interface tension in different states was calculated. Interface tension was usually obtained by the difference between the general and tangential stress on the integration interface. Based on the Irving-Kirkwood equation derived from Lyklema [22], the interface tension could be calculated [23, 24]:

$$\gamma = \int_0^x (p_n - p_t) dx \quad (13)$$

where p_n and p_t were normal pressure and tangential pressure, respectively among them, x represents the interface thickness.

Model verification

Often an analog system needed to verify that it was close to a real physical conformation based on the density of the system obtained by its kinetic calculations. In this regard, we simulated the structure of the lubricant molecular system. In the case of a system containing 300 frozen oil molecules, (288 K, 293 K, 298 K, 303 K, 308 K, 313 K) at 6 seconds were simulated using molecular dynamics density of the frozen oil system at temperature, as shown in fig. 2. The system density increases sharply with the simulation time, at which point the system volume will be reduced, the system density will remain basically the same after 30 ps simulation, and the system volume will remain basically constant, at this time the system is in a balanced and stable state.

In order to verify the accuracy of the simulation system and obtain accurate system density, volume, cohesion energy and solubility parameters, we compared the simulation and experimental results of the density of the frozen oil system with the temperature change. As shown in fig. 3, in the MD simulation, the system density at each temperature was averaged by the results calculated within 30-50 ps of the simulation time. At the same time, at 6 seconds (288 K, 293 K, 298 K, 303 K, 308 K, 313 K) for refrigeration oil density measurement experiments. As shown in fig. 3. At 288 K, the experimental density value is 0.799 g/cm³, the numerical simulation density is 0.797 g/cm³, and the numerical error does not exceed 2%. At the same time, it follows the curve rule in fig. 3. The lower the temperature, the smaller the error. The temperature difference will be smaller, so the MD simulation results were in good agreement with the experimental results, indicating that the constructed system could represent the real system and be applied to subsequent simulation calculations.

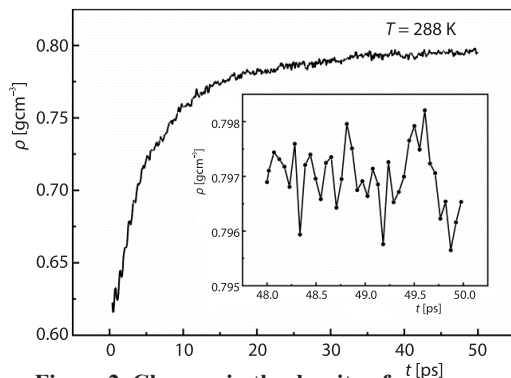


Figure 2. Changes in the density of refrigerating oil system over time

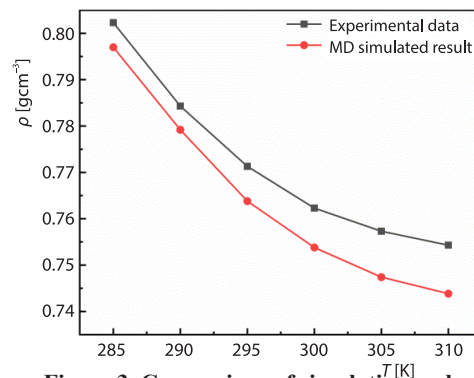


Figure 3. Comparison of simulation and experimental results of the density of refrigerating oil system with temperature

Results and discussion

Analysis of the influence of the interaction between ammonia and lubricating oil system

In oil/ammonia systems, the shape and stability of the interface depended on the concentration, and the nature of the interface was sensitive to changes in the temperature field. Therefore, the effect of temperature on behavior on the oil/ammonia interface could not be

ignored. In this simulation, the effect of different temperatures on the properties of the oil-water interface would be compared and analyzed by quantitative study of interface tension at equilibrium time. That was, the study of independent variable taking into account the volume ratio of different phases, the temperature was the focus of the detailed object. Among them, the analog phase volume ratio range was 10%, 30%, 50%, 70%, and 90%, and the system temperatures were 240 K, 245 K, 250 K, 255 K, and 260 K, respectively.

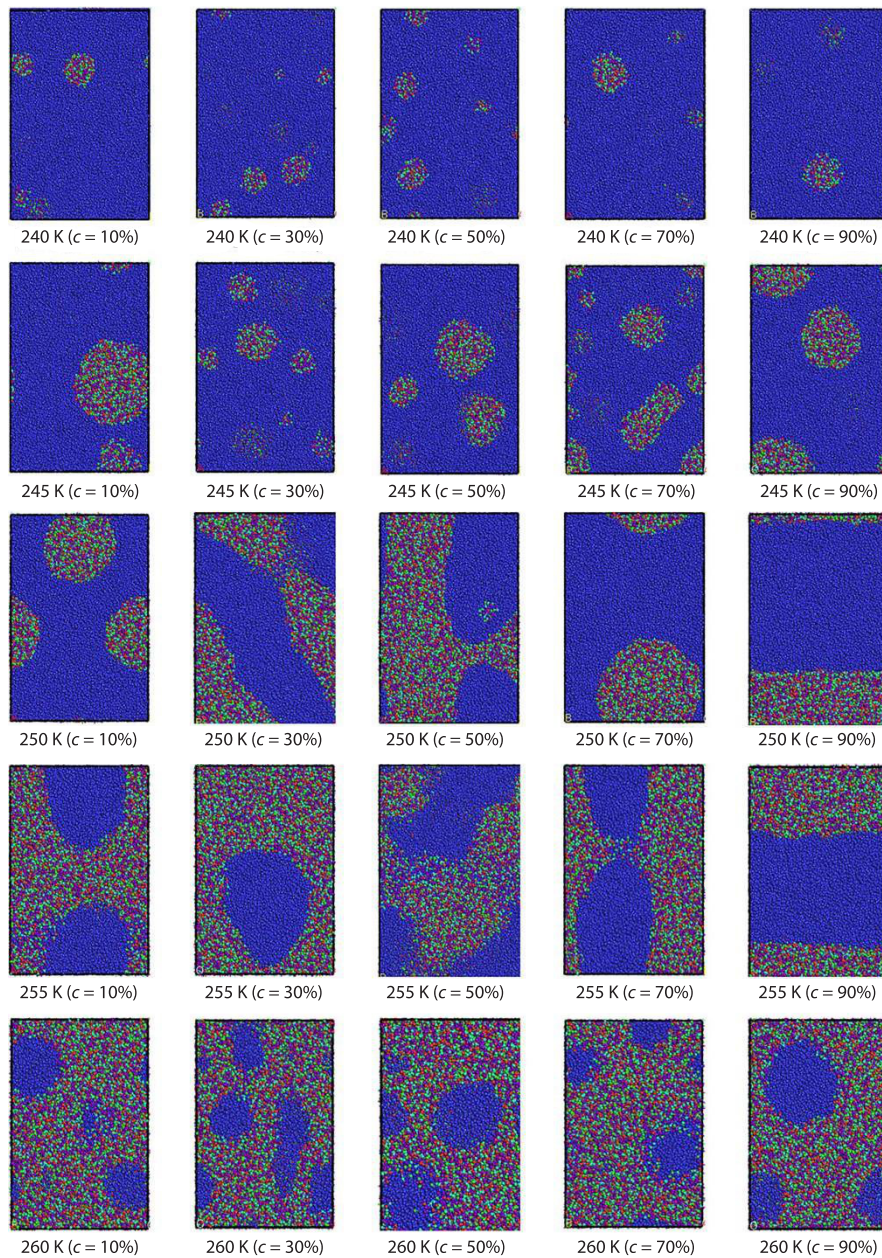


Figure 4. Changes in the volume ratio of different phases with different temperatures

As could be seen from fig. 4, at the same concentration, at 240 K temperature, oil/ammonia was present in the form of droplets. In addition 50% concentration, other concentrations increased with temperature, droplets were dispersed from dispersion aggregation, and then dispersed to aggregation, resulting in a stable form at 260 K temperatures. This was because at 50% concentration, the oil-ammonia system accounts for the same proportion, and the interaction effect of the factors, temperature occupies the main leading position, the concentration of less influence, would not lead to multiple recombination of a certain phase, and the distance between the beads was short, mostly within the stage radius. At a concentration of 30%, the droplets had a reverse law, which was due to the large initial liquid ammonia aggregation state. At concentrations of 50%, 70%, and 90%, the system has a compound of ammonia encapsion and oil-encapsion encapsion double emulsion structure. At $c = 10\%$ and $c = 90\%$, it could be seen that when the oil-ammonia ratio was 1:9 and 9:1, the diameter of the droplet was greater than the diameter of the oil droplet. according to the work of Scatena, *et al.* [25]. could be seen that there was a weak hydrogen bond between the liquid ammonia molecules at the oil-water interface, which resulted in the number of bits of liquid ammonia molecules on the interface was less than the number of bits of liquid ammonia molecules in the liquid ammonia phase. Therefore, the content of liquid ammonia-encapsulating emulsion droplets was less than that of oil-encapsulating type emulsions. So when the oil water was the same, the droplets had a larger volume.

In order to quantitatively explored the law of oil/ammonia flow state, we calculated the interface tension in different states, as shown in fig. 5. Interface tension changes with the change of oil-ammonia system shape, the maximum surface tension is about 250 K, in the oil content of 10%, 30%, and 90%, all three cases are emulsion state, and the corresponding interface tension increases with temperature. This was because molecules were heated to expand, and the oil molecular system becomes larger. Because there were hydrogen bonds in liquid ammonia, so the volume of liquid ammonia was not affected by temperature, so the oil content of 10% interface tension was flat than 90%. The oil content of 30% was abnormal at the beginning, because 30% was the transition point of the emulsion, the first part of the motion law was similar to the two-phase fluid motion law. At the oil content at 50% and 70%, the system clutter gradually became a stable layered state, where the interface was layered with two-phase fluids. As the temperature rises, the droplet began to break down and then regroup to form a stable layer, in which the temperature increased to provide energy to the oil molecules, thus changing the motion of the beads. The model interfaced with a 70% oil content at any temperature The force was greatest, because the 70% oil content and the oil content of 30% are reversed, because the proportion of ammonia is small, resulting in a larger degree of oil relative to liquid ammonia layer extrusion, ammonia-oil surface contact area became larger. And the presence of hydrogen bonds in the ammonia system, the greater the forced to destroy the ammonia phase.

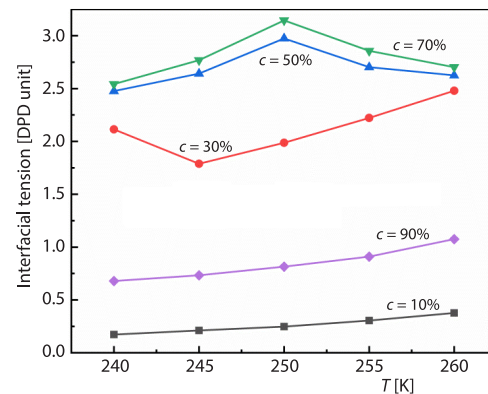


Figure 5. Interfacial tension changes with temperature

According to the aforementioned research results, we also found that the interface effects produced by different phase volume ratios are different. In order to explore the influence

of discrete phase volumes on the oil/ammonia interface, we analyzed the oil/ammonia system model at 260 K. The type of emulsion formed in a system is related to the phase volume [26]. By simulating the oil content of 10%, 30%, 50%, 70%, and 90%, the influence of different oil content on the structural changes of the oil-water emulsion system and the interface parameters is analyzed, as shown in fig. 6. The phase equilibrium diagram of the oil-water system with different oil content. It could be seen from the fig. 5 that the oil-ammonia emulsion will change from an oil-in-ammonia emulsion an oil-in-ammonia emulsion as the oil content gradually increases from 10-90%. When the oil content was 10%, the system is in the state of an oil-in-ammonia emulsion. At this time, the liquid ammonia phase is the continuous phase. When the oil content was 30%, the system was still in the state of an oil-in-ammonia emulsion. At this time, the oil droplets become larger and moved toward the wall at the same time, and the liquid phase interface becomes clearer. This point was the phase inversion point of the emulsion, which had a similar effect to the results of Plasencia *et al.* [27] In the inversion point, the system was in an unstable state, and the oil beads and liquid ammonia beads in the system will rearrange to find a new equilibrium state. When the oil content was 50-70%, the same type of oil beads and liquid ammonia beads were combined together to form a stable oil-ammonia two-phase system and a stable oil-ammonia two-phase interface. As the oil content increases, the interface contact area of the two-phase interface increases. This was caused by the increase of oil beads, and the interaction force of the oil bead system in the system gradually increases, resulting in deformation of the oil-water interface, and the interfacial tension would increase. When the oil content was 70-90%, the stable layered interface was damaged, forming an ammonia-in-oil system, and large liquid ammonia droplets would gradually be compressed into small droplets.

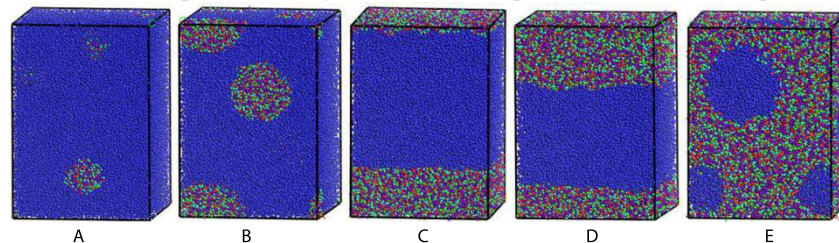


Figure 6. Equilibrium morphology of oil-ammonia system with different oil content at 260 K

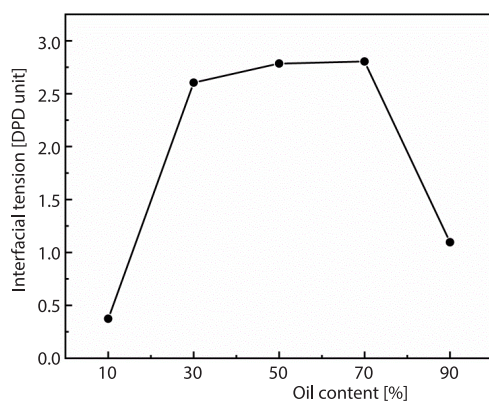


Figure 7. Change of interfacial tension with oil content

In order to verify the previous conclusions, we also calculated the corresponding interfacial tension, which can better explain the changes in the oil/ammonia system caused by the refrigerant phase change process in the evaporator, as showed in fig. 7. The interfacial tension increases first and then decreases with the oil concentration. This was similar to Dick [28] pointed out in the study of the surface tension of refrigerant-oil mixtures that the surface tension of the mixture first increased and then decreased with the increase of oil concentration. Similar conclusions. When the phase volume ratio was 70%, the heat transfer had the most impact. At this time, the interfacial tension got to the maximum and the interfaced contact area

reaches the maximum. The oil layer was distributed outside the liquid ammonia, closed to the wall, and hinders the heat transferred of the liquid ammonia. When the concentration of liquid ammonia was too low, the liquid ammonia was enveloped by oil, but the liquefied ammonia gradually vaporized in the evaporator, and the heat transfer effect was not as great as that of laminar flow. At the same time, before the concentration of 50%, the interfacial tension gradually increased and the heat transfer effected gradually deteriorates.

The improvement of the DPD parameterized model with temperature as a variable

Temperature had a certain influence on various parameters in the simulation process in previous research process. Therefore, we simulated the correspondence between the Flory-Huggins parameter χ and the excess repulsive force parameter Δa at different temperatures. and then applied them to calculate the repulsion parameters. This provided a data basis for the follow-up study to strengthen the refrigerant heat exchange of the ammonia refrigeration evaporator.

The influence of temperature on the conservative force parameters is considered, and the conservative force parameters $a(T)_{ii}$ between beads of the same species are calculated under the conditions of temperature 240 K, 245 K, 250 K, 255 K, and 260 K, respectively, as showed in tab. 2.

Table 2. Conservative force parameters between beads at different temperatures

T [K]	Vol_{ammonia} [\AA^3]	k_T [bar^{-1}]	$K^{-1}(k_B T)$	$a(T)_{ii} (k_B T/r_c)$
235	40.912	35.247	12.588	60.422
240	41.453	35.532	12.462	59.817
245	41.211	35.958	12.317	59.121
250	42.197	36.373	12.142	28.281
255	42.617	36.977	11.947	57.346
260	43.039	37.679	11.716	56.237

For liquid ammonia with temperatures of 235 K, 240 K, 245 K, 250 K, 255 K, and 260 K, as the temperature increased, the repulsive force $a(T)_{ii}$ between the same kind of beads decreased. This was because the increase in temperature causes the volume of the system to expand and at the same time the compressibility of the system is increased. According to the description of the conservative force between the same kind of beads according to the following formula, the moderate force between the beads in the system will be reduced accordingly.

The Flory-Huggins parameter has a linear relationship with the conservative force parameter difference Δa between different particles. Groot and Warren [29] established the relationship eq. (12) between the Flory-Huggins parameter and the conservative force parameter through theoretical calculations. In the lattice model, the volume fractions of molecules A and B are ϕ_A and $\phi_B = 1 - \phi_A$, respectively. If the A bead represents a polymer molecule containing N_A fragments and the B bead represents a solvent molecule containing N_B fragments, the free energy in each lattice can be written:

$$\frac{f_V}{k_B T} = \frac{\phi_A}{N_A} \ln \phi_A + \frac{\phi_B}{N_B} \ln \phi_B + \chi \phi_A \phi_B \tag{14}$$

For a multi-component system, the repulsion parameter a_{ij} between different beads could be calculated by their solubility in water. Among them, the Flory-Huggins parameter χ and Δa ($\Delta a = a_{ij} - a_{ww}$) satisfy the linear relationship [30-32]:

$$\chi = \lambda \Delta a \quad (15)$$

This DPD method was used to regress the linear relationship equation between χ and Δa at different temperatures. In the simulation, the grid size was set to $200 \times 100 \times 100 \text{ \AA}^3$, which contained 3000 A beads and 3000 B beads.

When the system was in equilibrium, the average volume percentage of each bead at the AB bead interface in the system was taken as the independent variable, and the corresponding Flory-Huggins parameters at each temperature could be obtained by eqs. (11)-(15). Then fit the linear relationship equation between χ and Δa and its relationship diagram, as showed in fig. 8. We had obtained the volume and solubility parameters of the molecular system at a temperature of 240 K before. In order to explore the influence of different temperatures on the system, we carried out simulation calculations based on the previous formula, and obtained the simulation results of the molecular solubility parameters and mixing free energy at different temperatures, which are listed in fig. 9 and tab. 3, respectively. For the convenience of research, the following collectively referred to as propyl for $-(C_3H_6)-$ and $(C_3H_7)-$.

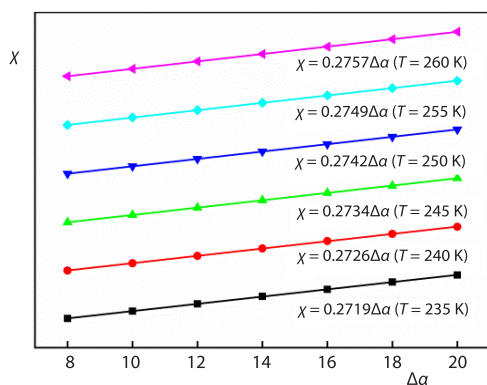


Figure 8. Linear relationship equation between χ and Δa

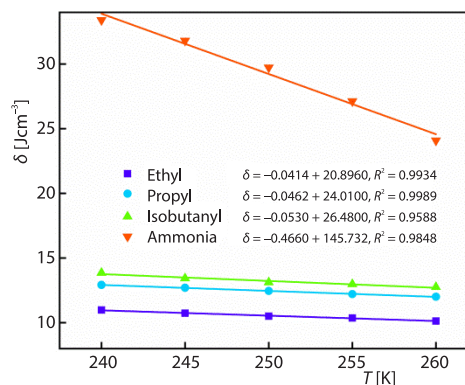


Figure 9. Changes of solubility parameters with temperature

Table 3. Mixing free energy at different temperatures

T [K]	E_{mix} [kcalmol ⁻¹]					
	Ethyl/ propyl	Ethyl/ isobutanyl	Ethyl/ ammonia	Propyl/ isobutanyl	Propyl/ ammonia	Isobutanyl/ ammonia
240 K	0.440	0.633	17.658	0.291	12.621	21.071
245 K	0.380	0.654	17.601	0.264	19.619	20.700
250 K	0.362	0.616	17.340	0.198	19.323	20.401
255 K	0.329	0.598	17.038	0.154	19.074	20.123
260 K	0.268	0.538	16.582	0.128	18.769	19.862

Table 3 showed the variation of free energy of mixing of liquid ammonia, ethyl, propyl and isobutylene systems in the simulated system with temperature. It could be seen from tab. 3 that the free energy of mixing also decreased with increasing temperature.

Among them, due to the strong hydrogen bond between the liquid ammonia and the charged structure, compared with the decrease of the mixing free energy of other components with the temperature, the decrease will increase. The reason was perhaps that the existence of hydrogen bonds will reduce the mutual solubility of different compounds. However, this also meant that the interaction caused by the destruction of hydrogen bonds requires more energy to the system. For a two-component mixed system, the calculation results of Flory-Huggins parameters with temperature changes were shown in fig. 10. The initial property parameters (solubility parameter and free energy of mixing) required for this calculation use the MD simulation results listed in fig. 11 and tab. 3. It could be observed from the fig. 11 that the relationship between χ and $1/T$ was in line with the description of the influence of temperature on the parameters of Flory-Huggins in the Flory-Huggins theory. Figure 11 showed the calculation results of conservative force parameters between DPD beads. It could be seen from the figure that the change of the conservative force parameter, a_{ij} , with temperature is approximately a linear decrease.

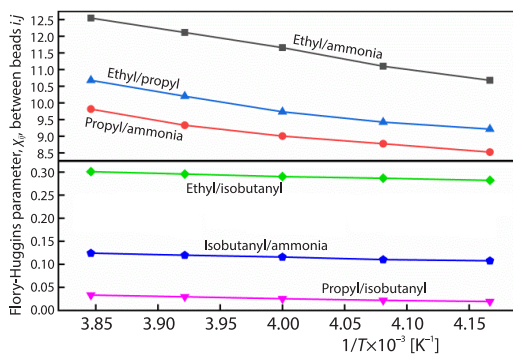


Figure 10. Changes of Flory-Huggins parameter with temperature

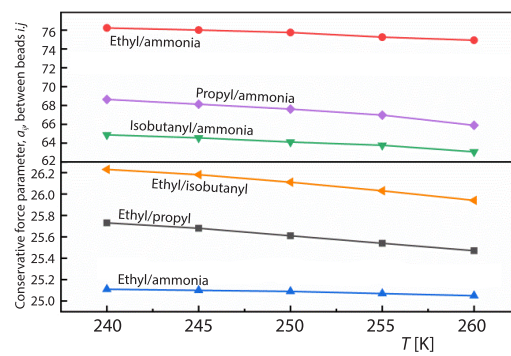


Figure 11. Changes of conservative force parameter, a_{ij} , with temperature

Conclusion

The state of the refrigerating oil and refrigerant system models were different at different temperatures, and the liquid phases with low content at low temperatures were all stored in the form of droplets. When the oil-ammonia ratio was 1:9 and 9:1, the diameter of liquefied ammonia droplets was larger than that of oil droplets due to the existence of hydrogen bonds, and the interfacial tension increases with temperature. At the same temperature, the interfacial tension was maximum when the oil content was 70%. The liquid phase with minimal content at low temperature exists in the form of droplets. At the same temperature, the oil-ammonia interfacial tension first increases and then decreased with the increase in oil content. The effect of oil content on the two-phase system could be divided into an emulsion and layered liquid. Oil-ammonia interfacial tension first increased and then decreased with the increase in oil content. The oil content of 30% concentration is the phase inversion point. At the phase inversion point, the system was in an unstable state. At that time, the oil beads and liquid ammonia beads in the system would be rearranged to find a new equilibrium form. The influence of temperature on various parameters in the liquid ammonia-oil system was studied. The DPD rejection parameter a_{ij} had been calculated through a modified function relationship with the Flory-Huggins parameter χ at different temperatures. The simulation results were further verified by experiments. As the temperature increases, calculated interaction parameter a_{ij} decreases significantly. In

addition, the linear relationship between χ and $1/T$ was quite consistent with the Flory-Huggins mean field theory. These data could provide reference for our follow-up research on the modification of ammonia refrigeration.

Acknowledgment

This work was supported by National Nature Science Foundation of China (Grant No. 52076036) and Natural Science Foundation of Heilongjiang Province (Grant No. LH2020E017).

References

- [1] Zhang, Q. R., et al., Optimization Analysis of Air-Flow Organization when Ammonia Leaks in a Refrigeration Room, *Journal of Refrigeration*, 42 (2021), 1, pp. 36-44
- [2] Bao, J. H., et al., The Research Status and Problems of Natural Working Fluid, *Refrigeration*, 152 (2020), 3, pp. 40-47
- [3] Zhang, Y., Optimization Design of Liquid Ammonia Storage Tank Process in Ammonia Refrigeration System, *Contemporary Chemical*, 50 (2021), 1, pp. 237-239
- [4] Chen, R., et al., A Review of Research on the Influence of Lubricating Oil with Poor Mutual Solubility with Working Fluids on Refrigeration Systems, *Fluid Machinery*, 47 (2019), 10, pp. 64-70
- [5] Qiu, L. Z., *Research on the Performance and Boiling Heat Transfer Characteristics of R32/Lubricating Oil Mixture*, Shanghai Jiao Tong University, Shanghai, China, 2020
- [6] Chu, W., et al., A Review on Experimental Investigations of Refrigerant/Oil Mixture Flow Boiling in Horizontal Channels, *Applied Thermal Engineering*, 196 (2021), 117270
- [7] Wang, Y., et al., Study on Characteristics of Fluid-Flow and Heat Transfer in the Torsional Flow Heat Exchanger with Drop-Shaped Tube, *Thermal Science*, 26 (2021), 5A, pp. 3689-3702
- [8] Asim, M., et al., Flow Boiling Heat Transfer Characteristics of Low GWP Refrigerants in a Vertical Mini-Channel, *Thermal Science*, 26 (2022), 1A, pp. 63-76
- [9] Jing, Q., et al., Experimental Study on the Correlation of Subcooled Boiling Flow in Horizontal Tubes, *Thermal Science*, 26 (2022), 1A, pp. 107-117
- [10] Hou, W., Talking About the Influence of Lubricant Failure on Ammonia Compression Refrigeration System, *Science and Technology Innovation Herald*, 4 (2011), pp. 89-89
- [11] Ginzburg, V. V., et al., Modelling the Interfacial Tension in Oil-Water-Non-Ionic Surfactant Mixtures Using Dissipative Particle Dynamics and Self-Consistent Field Theory, *Journal of Physical Chemistry B*, 115 (2011), 16, pp. 4654-1661
- [12] Yao, W., et al., Dissipative Particle Dynamics Simulation of Droplet Motion Characteristics on Structured Wall, *Journal of Physics*, 62 (2013), 13, pp. 355-361
- [13] Mayoral, E., et al., Modelling of Branched Thickening Polymers under Poiseuille Flow Gives Clues as to How to Increase a Solvent's Viscosity, *The Journal of Physical Chemistry B*, 125 (2021), 6, pp. 1692-1704
- [14] Li, Y., et al., Dissipative Particle Dynamics Simulation on the Properties of the Oil/Water/Surfactant System in the Absence and Presence of Polymer, *Molecular Simulation*, 39 (2013), 4, pp. 299-308
- [15] Liu, H. Y., et al., Computer Simulations on the Anticancer Drug Delivery System of Docetaxel and PL-GA-PEG Copolymer, *Acta Chimica Sinica*, 70 (2012), 23, pp. 2445-2450
- [16] Hansen, C. M., *Hansen Solubility Parameters: A User's Handbook*, CRC Press, Boca Raton, Fla., USA, 2002
- [17] Goodarzi, F., et al., Effects of Salt and Surfactant on Interfacial Characteristics of Water/Oil Systems: Molecular Dynamic Simulations and Dissipative Particle Dynamics, *Industrial and Engineering Chemistry Research*, 58 (2019), 20, pp. 8817-8834
- [18] Rekvig, L., et al., Investigation of Surfactant Efficiency Using Dissipative Particle Dynamics, *Langmuir*, 19 (2003), 20, pp. 8195-8205
- [19] Oliveira, F. C., et al., Asphaltene at the Water-Oil Interface Using DPD/COSMO-SAC, *Colloids and Surfaces A: Physicochemical and Engineering Aspects*, 625 (2021), 12682
- [20] Yang, S. W., *Research on the Properties of Surfactant Oil-Water Interface Based on the Dynamics of Dissipative Particles*, Northeast Petroleum University, Daqing, China, 2020
- [21] Wang, Y., et al., A New Model for Dissipative Particle Dynamics Boundary Condition of Walls with Different Wettabilities, *Applied Mathematics and Mechanics: English Version*, 42 (2021), 4, pp. 467-484
- [22] Lyklema, J., *Fundamentals of Interface and Colloid Science: Soft Colloids*, Elsevier, Amsterdam, The Netherlands, 2005

- [23] Maiti, A., *et al.*, Bead-Bead Interaction Parameters in Dissipative Particle Dynamics: Relation Bead-Size, Solubility Parameter, and Surface Tension, *Journal of Chemical Physics*, 120 (2004), 3, pp. 1594-1601
- [24] Yang, S. W., *et al.*, Numerical Simulations of the Effect of Ionic Surfactant/Polymer on Oil-Water Interface Using Dissipative Particle Dynamics, *Asia-Pacific Journal of Chemical Engineering*, 11 (2016), 4, pp. 581-593
- [25] Scatena, L. F., *et al.*, Water at Hydrophobic Surfaces: Weak Hydrogen Bonding and Strong Orientation Effects, *Science*, 292 (2001), 5518
- [26] Fatemeh, G., *et al.*, Effects of Salt and Surfactant on Interfacial Characteristics of Water/Oil Systems: Molecular Dynamic Simulations and Dissipative Particle Dynamics, *Industrial and Engineering Chemistry Research*, 58 (2019), Mar., pp. 8817-8834
- [27] Plasencia J., *et al.*, Pipe Flow of Water-in-Crude-Oil Emulsions Effective Viscosity, Inversion Point and Droplet Size Distribution, *Journal of Petroleum Science and Engineering*, 11 (2013), 1, pp. 35-43
- [28] Dick, H. G., *et al.*, Heat Transfer to Boiling Refrigerant-Oil Mixtures, *Proc. Int. Cong. Refrig.*, 2 (1975), pp. 351-359
- [29] Groot, R. D., *et al.*, Dissipative Particle Dynamics: Bridging the Gap between Atomistic and Mesoscopic Simulation, *The Journal of Chemical Physics*, 107 (1997), 11, pp. 4423-4435
- [30] Goodarzi, F., *et al.*, Effects of Salt and Surfactant on Interfacial Characteristics of Water/Oil Systems: Molecular Dynamic Simulations and Dissipative Particle Dynamics, *Industrial and Engineering Chemistry Research*, 58 (2019), 20, pp. 8817-8834
- [31] Wu, J. Z., *et al.*, Dissipative Particle Dynamics of Asphaltene Molecular Interface Behavior, *Acta Petrolei Sinica (Petroleum Processing Section)*, 37 (2021), 5, pp. 1106-1113
- [32] Oliveira, F., *et al.*, Asphaltenes at the Water-Oil Interface Using DPD/COSMO-SAC, *Colloids and Surfaces A Physicochemical and Engineering Aspects*, 625 (2021), 126828